Improved Models of Stellar Core Collapse and Still No Explosions: What Is Missing?

R. Buras, M. Rampp, H.-Th. Janka, and K. Kifonidis
Max-Planck-Institut für Astrophysik, Karl-Schwarzschild-Strasse 1, D-85741 Garching, Germany
(Received 7 March 2003; published 19 June 2003)

Two-dimensional hydrodynamic simulations of stellar core collapse are presented which for the first time were performed by solving the Boltzmann equation for the neutrino transport including a state-of-the-art description of neutrino interactions. Stellar rotation is also taken into account. Although convection develops below the neutrinosphere and in the neutrino-heated region behind the supernova shock, the models do not explode. This suggests missing physics, possibly with respect to the nuclear equation of state and weak interactions in the subnuclear regime. However, it might also indicate a fundamental problem with the neutrino-driven explosion mechanism.

DOI: 10.1103/PhysRevLett.90.241101 PACS numbers: 97.60.Bw, 26.50.+x, 95.30.Jx, 95.30.Lz

Despite more than three decades of theoretical research and numerical modeling, the processes which cause the explosion of massive stars are still not understood. Current observational data of supernovae (SNe) do not provide direct information. Although neutrinos (ν) and gravitational waves could yield such insight, the ν events detected in connection with SN 1987A were too sparse to constrain the SN mechanism. Progress in our understanding of the complex phenomena in collapsing stars and nascent ("proto-") neutron stars (PNSs) is therefore mainly based on hydrodynamic simulations.

Stars more massive than about ten solar masses ($M_\odot$) develop an iron core in a sequence of nuclear burning stages. This iron core becomes gravitationally unstable when it reaches a mass close to its Chandrasekhar limit and collapses to a neutron star. A hydrodynamic shock forms when nuclear density is reached and the matter becomes incompressible. There is general agreement, supported by detailed numerical models, that this shock is not able to promptly cause a SN explosion. Instead, it suffers from severe energy losses by the photodisintegration of iron nuclei to free nucleons. It finally stalls after having reached densities low enough that electron neutrinos (ν_e) can rapidly escape in a luminous outburst and thus drain even more energy from the shock-heated matter [1–3].

While ν losses damp the shock in this early phase, the situation changes some 50 ms later. As more stellar matter falls onto the collapsed inner core, the shock is pushed to larger radii and the density and temperature behind the shock decrease. On the other hand, the central core begins to settle and heats up, thus radiating more energetic neutrinos. Both effects lead to the situation that ν_e and $\bar{\nu}_e$ can now be absorbed with a small probability (10%–20%) by free neutrons and protons behind the shock. A region of ν heating between the so-called "gain radius" and the shock front develops [4]. If the ν energy deposition is efficient enough, the stalled shock can be revived and drives a "delayed" explosion.

The success of pioneering calculations [4] could be maintained in later models only by invoking neutron-finger convective instabilities in the PNS [5]. These boost the ν luminosities and thus enhance the ν-energy transfer to the shock. Explosion energies similar to those of observed SNe required even higher ν fluxes. It was proposed that these could be obtained when pions appear in large numbers in the PNS matter [6]. The existence of neutron-finger instabilities, however, depends on very specific thermodynamical properties of the equation of state (EOS) and on the details of the ν transport [7]. The formation of pions in hot PNS matter, on the other hand, is highly uncertain and requires particular assumptions about their dispersion relation.

While all simulations addressed so far were performed in one dimension (1D) assuming spherical symmetry (neutron-finger convection was treated by a mixing-length approach), SN 1987A provided evidence for large-scale mixing processes which carried radioactive nuclei from the region of their formation near the PNS into the helium and hydrogen shells of the exploding star. Simulations suggested that their origin may be linked to hydrodynamic instabilities behind the stalled shock already during the first second of the explosion [8]. Two-dimensional (2D) [9] and most recently also three-dimensional (3D) [10] models that take into account ν effects then showed that convective overturn indeed develops in the ν heating region and is helpful for shock revival, thus making explosions possible even when spherically symmetric models fail [11].

The multidimensional situation is generically different because it allows accretion to continue while shock expansion already sets in. Narrow downflows bring cold, low-entropy matter close to the gain radius, where the ν energy deposition is strongest. At the same time heated matter can rise in buoyant bubbles, thus pushing the shock farther out and reducing energy loss by the reemission of neutrinos. Although this increases the efficiency of ν-energy transfer, convection is still no guarantee that explosions occur [11]. A particular concern with all multidimensional models which yielded explosions was the much simplified treatment of the ν transport by grey diffusion schemes, which was inferior to the more

elaborate multigroup transport description used in unsuccessful spherical models [12].

Recently it has become possible to go a step further and solve the time-dependent Boltzmann equation for ν transport in 1D hydrodynamic simulations with Newtonian [13–15] and relativistic gravity [16]. It turned out that even this improvement does not lead to explosions. The question, however, remained whether convection might bring the models to success. Here we present the first 2D simulations which were performed with a Boltzmann solver for the ν transport. At the same time we have also upgraded the description of ν-matter interactions compared to the conventional treatment of Refs. [1,17,18].

Numerical techniques and input physics.—For the integration of the equations of hydrodynamics we employ the Newtonian finite-volume code PROMETHEUS [19]. This second-order, time-explicit Godunov scheme is a direct Eulerian implementation of the piecewise parabolic method [20] and is based on a Riemann solver.

The Boltzmann solver scheme for ν and $\bar{\nu}$ of all three flavors is described in detail in Ref. [18]. In multidimensional simulations in spherical coordinates, we solve for each latitude θ of the numerical grid the monochromatic moment equations for the radial transport of the ν number, energy, and momentum. This set of equations is closed by a variable Eddington factor that is calculated from the solution of the Boltzmann equation on an angularly averaged stellar background. In addition, we had to go an important step beyond this "ray-by-ray" approximation of multidimensional transport. Physical constraints, namely, the conservation of lepton number and entropy within adiabatically moving fluid elements and the stability of regions which should not develop convection according to a stability analysis, made it necessary to take into account the coupling of neighboring rays at least by lateral advection terms and ν pressure gradients [21].

General relativistic effects are treated approximately by modifying the gravitational potential with correction terms due to pressure and energy of the stellar medium and neutrinos, which are deduced from a comparison of the Newtonian and relativistic equations of motion [18]. The ν transport contains gravitational redshift and time dilation, but ignores the distinction between coordinate radius and proper radius. This is necessary for coupling the transport code to our basically Newtonian hydrodynamics. Comparison with fully relativistic 1D simulations showed that these approximations work well at least when the deviations of the metric coefficients from unity are moderate [22].

Improving the description of ν interactions [21] compared to the "standard" opacities [1,17] we added ν-pair creation (and annihilation) by nucleon-nucleon bremsstrahlung [23], scattering of ν_μ, $\bar{\nu}_\mu$, ν_τ, and $\bar{\nu}_\tau$ off ν_e and $\bar{\nu}_e$, and pair annihilation reactions between neutrinos of different flavors [24]. We also take into account the detailed reaction kinematics with nucleon thermal motions, recoil, and fermion phase-space blocking effects in the charged- and neutral-current ν-nucleon interactions. Moreover, nuclear correlations [25], weak-magnetism corrections [26], and the reduction of the nucleon effective mass and possible quenching of the axial-vector coupling in nuclear matter [27] are included, too.

Our current SN models are calculated with the EOS of Ref. [28] using an incompressibility of bulk nuclear matter of 180 MeV (other values make only minor differences [15]). This EOS is based on a compressible liquid-drop model including nuclei, nucleons, e^-, e^+, and photons.

The 2D simulations were performed with a spherical coordinate grid with about 400 radial zones and assuming azimuthal symmetry around the polar axis. A wedge of roughly 90° was chosen in the angular direction between the angles θ_0 and θ_1 and with the number of mesh points, N_θ, as given in Table I. For the nonrotating models periodic boundary conditions were taken. For the rotating model reflecting boundaries at the axis and the equator were imposed.

We considered three (solar metallicity) progenitors with main sequence masses of $11.2M_\odot$, $15M_\odot$, and $20M_\odot$ [29]. The model specific parameters are given in Table I. For the transport we used an energy grid of 17 geometrically spaced bins with centers from 2 to 333 MeV. Higher energy resolution was tested without giving significant differences. Model s15p is a calculation where random density perturbations with 1% amplitude were imposed on the precollapse core to follow their growth during infall [30]. In the rotating model s15r the angular frequency was assumed to be constant in the Fe and Si core and decreasing as $r^{-3/2}$ outside of 1750 km ($1.43M_\odot$). These choices and the adopted rotation rate (cf. Table I) are basically in agreement with predictions from stellar evolution models [31].

Results.—Convective overturn starts to appear in the region of ν heating behind the shock about 25 ms after

TABLE I. Parameters of computed 2D models for progenitor stars with different masses. $M_{\rm Fe}$ is the iron core mass, $M_{\rm Si+O}$ the mass interior to the inner edge of the oxygen-rich Si shell, $\Omega_{\rm i}$ the angular velocity of the Fe core prior to collapse, θ_0 and θ_1 are the polar angles of the lateral grid boundaries, and N_θ is the number of grid points in the lateral direction.

Model	Mass ($M_\odot$)	$M_{\rm Fe}$ ($M_\odot$)	$M_{\rm Si+O}$ ($M_\odot$)	$\Omega_{\rm i}$ (s^{-1})	$[\theta_0, \theta_1]$ (degrees)	N_θ
s11.2	11.2	1.24	1.30	0	[46.8, 133.2]	32
s11.2	11.2	1.24	1.30	0	[46.8, 133.2]	64
s15	15	1.28	1.43	0	[46.8, 133.2]	32
s15p	15	1.28	1.43	0	[46.8, 133.2]	64
s15r	15	1.28	1.43	0.5	[0, 90]	64
s20	20	1.46	1.46	0	[46.8, 133.2]	32

shock formation, and begins to affect the SN dynamics about 50 ms later. Expanding bubbles of heated matter deform the shock (Fig. 1) and lead to a transient increase of the average shock radius (Fig. 2). The difference to spherically symmetric simulations, however, is small in the case of models s15 and s20, because the convectively unstable layer between gain radius and shock remains narrow and the overturn motions never become very strong. The largest relative change occurs when the big entropy discontinuity at the inner boundary of the oxygen enriched shell ($M_{\mathrm{Si+O}}$, Table I) of the progenitor star crosses the shock. The sudden decrease of the density and ram pressure of the infalling matter allows the shock to transiently expand also in 1D simulations. In model s11.2 the corresponding growth of the shock radius is nearly 50 km. This in turn widens the gain layer and thus allows convection to strengthen. The combined effects lead to a much larger shock radius than in the 1D case (Fig. 2). A similar result is caused by centrifugal forces in the rotating model s15r (Fig. 2). Here decelerated infall of matter near the equatorial plane and a reduced density near the poles create a more favorable situation for violent convection (Fig. 1).

Ledoux convection sets in *below* the neutrinosphere already about 40 ms after bounce. It is persistent until the end of our simulations and slowly digs farther into the star (cf. Fig. 1, lower left panel) in agreement with previous 2D simulations [32]. But the active layer is rather deep inside the PNS (at a density above 10^{12} g cm^{-3}) and is surrounded by a convectively stable shell in which the surface fluxes of ν_e and $\bar{\nu}_e$ are mainly built up. Therefore

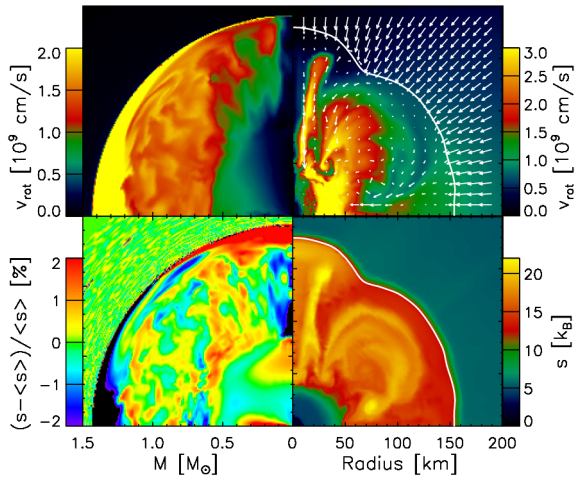

FIG. 1 (color online). Snapshots of the stellar structure for the rotating model s15r at 198 ms after shock formation. The left panels show the rotational velocity (top) and the fluctuations of entropy (in per cent) versus the enclosed mass, emphasizing the conditions inside the neutron star. The right panels display the rotational velocity (top) and the entropy (in k_{B} per nucleon) as functions of radius. The arrows indicate the velocity field, the white line marks the shock front.

the PNS convection has little influence on the emission of these neutrinos and is irrelevant for the SN dynamics. The differences in the ν_e and $\bar{\nu}_e$ luminosities and mean energies relative to the 1D case (Fig. 3) are caused by rotation and matter downflows from the shock to the neutrinospheric region. These accretion flows dominate the latitudinal variation of the ν emission because the rotational deformation of the PNS is moderate (Fig. 1).

Random density perturbations in the progenitor (model s15p) increase in the supersonically infalling layers and are damped in the subsonically collapsing inner core as predicted by linear analysis [30]. We have not discovered any influence on the development of convection. Also the shock radii of models s15p and s15 are nearly identical. Higher angular resolution allows convection to grow somewhat faster because of reduced numerical viscosity. Within the limits of our tests the later evolution in cases of strong convection exhibits quantitative but no qualitative differences (see model s11.2 in Fig. 2).

Conclusions.—It is shown that an accurate treatment of the neutrino physics does not yield sufficiently efficient ν-energy transfer behind the stalled SN shock to produce explosions, even though convection occurs below the neutrinosphere and in the ν-heating region. This finding confirms concerns [12] that the success of previous models [9] was favored by gross simplifications of the ν transport.

None of the included effects is therefore able to cause explosions. Truly multidimensional transport [21] or full relativity [22] are not likely to change the situation. But the long-time evolution of the shock is sensitive to the ν emission that originates from the neutrinospheric layer. The EOS properties and ν interactions at densities below some 10^{13} g cm^{-3} are therefore particularly relevant. The structure, temperature, and convective stability of this layer depend also on the compactness of the PNS and thus

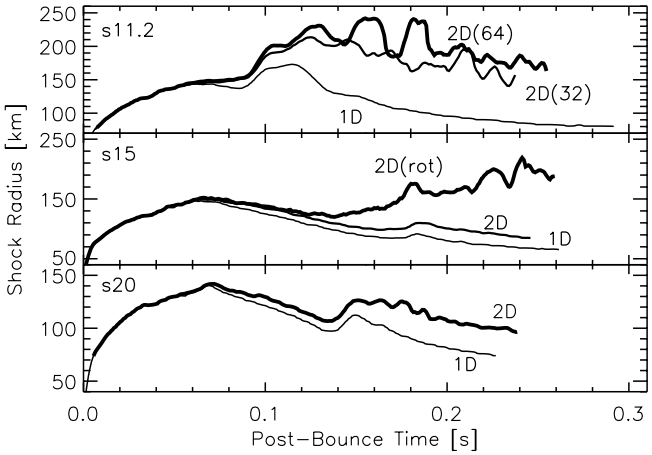

FIG. 2. Shock radii (averaged over polar angles) vs post-bounce time. The 2D models (bold lines) are compared to the corresponding 1D simulations (thin lines).

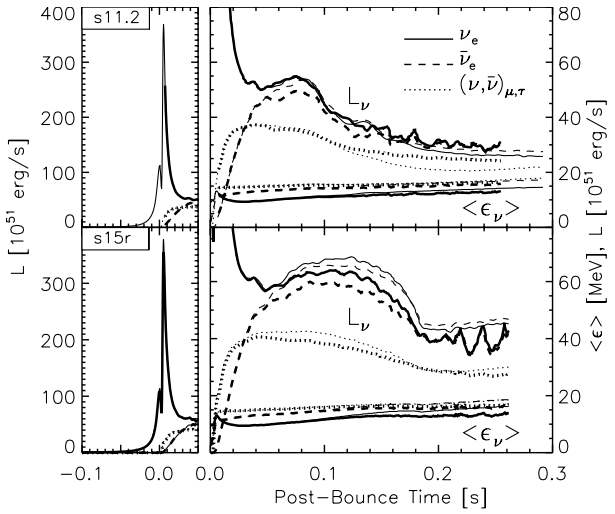

FIG. 3. Luminosities and mean energies (defined as the ratio of energy flux to number flux) for ν_e, $\bar{\nu}_e$ and $\nu_{\mu,\tau}$, $\bar{\nu}_{\mu,\tau}$ vs time for models s11.2 (top) and s15r (measured by an observer comoving with the stellar medium at 500 km). The left panels (left scale) show the prompt ν_e burst; the right panels enlarge the postbounce evolution. The thin lines represent results of 1D simulations for comparison.

on the uncertain physics in its supranuclear core. The influence of the EOS on the postbounce dynamics, however, has not been explored extensively so far. Necessary improvements of weak interactions on nuclei include electron capture rates [33] and inelastic neutrino scattering. Moreover, our 90° latitudinal wedge precludes the growth of an $l = 1$ mode instability, and generically 3D phenomena cannot be studied with 2D hydrodynamics.

The current paradigm for explaining massive star explosions would have to be revised if the ν-driven mechanism were fundamentally flawed. SNe might be aided by, e.g., magnetohydrodynamic processes [34] or even more exotic physics. Although it is still too early for this conclusion, such investigations deserve more interest.

We are indebted to K. Takahashi and C. Horowitz for help in improving ν-nucleon interactions. Support by the Sonderforschungsbereich 375 on "Astroparticle Physics" of the Deutsche Forschungsgemeinschaft is acknowledged. The simulations were done on the IBM "Regatta" supercomputer of the Rechenzentrum Garching.

[1] S.W. Bruenn, Astrophys. J. Suppl. Ser. **58**, 771 (1985).
[2] S.W. Bruenn, Astrophys. J. **340**, 955 (1989); **341**, 385 (1989).
[3] E. S. Myra *et al.*, Astrophys. J. **318**, 744 (1987); E. S. Myra and S. A. Bludman, Astrophys. J. **340**, 384 (1989).
[4] J. R. Wilson, in *Numerical Astrophysics*, edited by J. M. Centrella *et al.* (Jones and Bartlett, Boston, 1985), p. 422; H. A. Bethe and J. R. Wilson, Astrophys. J. **295**, 14 (1985).
[5] J. R. Wilson and R. Mayle, Phys. Rep. **163**, 63 (1988); **227**, 97 (1993).
[6] R.W. Mayle, M. Tavani, and J. R. Wilson, Astrophys. J. **418**, 398 (1993).
[7] S.W. Bruenn and T. Dineva, Astrophys. J. Lett. **458**, L71 (1996).
[8] M. Herant, W. Benz, and S. A. Colgate, Astrophys. J. **395**, 642 (1992).
[9] A. Burrows, J. Hayes, and B. A. Fryxell, Astrophys. J. **450**, 830 (1995); M. Herant, W. Benz, W. R. Hix, C. L. Fryer, and S. A. Colgate, Astrophys. J. **435**, 339 (1994); C. L. Fryer, Astrophys. J. **522**, 413 (1999); C. L. Fryer and A. Heger, Astrophys. J. **541**, 1033 (2000).
[10] C. L. Fryer and M. S. Warren, Astrophys. J. Lett. **574**, L65 (2002).
[11] H.-T. Janka and E. Müller, Astron. Astrophys. **306**, 167 (1996).
[12] A. Mezzacappa *et al.*, Astrophys. J. **495**, 911 (1998).
[13] A. Mezzacappa *et al.*, Phys. Rev. Lett. **86**, 1935 (2001).
[14] M. Rampp and H.-T. Janka, Astrophys. J. Lett. **539**, L33 (2000).
[15] T. A. Thompson, A. Burrows, and P. A. Pinto, astro-ph/0211194.
[16] M. Liebendörfer *et al.*, Phys. Rev. D **63**, 103004 (2001).
[17] A. Mezzacappa and S.W. Bruenn, Astrophys. J. **405**, 637 (1993); **410**, 740 (1993).
[18] M. Rampp and H.-T. Janka, Astron. Astrophys. **396**, 361 (2002).
[19] B. A. Fryxell, E. Müller, and W. D. Arnett, MPI Report No. MPA-449, 1989.
[20] P. Colella and P. R. Woodward, J. Comput. Phys. **54**, 174 (1984).
[21] R. Buras, M. Rampp, H.-T. Janka, K. Kifonidis, K. Takahashi, and C. J. Horowitz (to be published).
[22] M. Liebendörfer, M. Rampp, H.-T. Janka, and A. Mezzacappa (to be published).
[23] S. Hannestad and G. Raffelt, Astrophys. J. **507**, 339 (1998).
[24] R. Buras, H.-T. Janka, M.-T. Keil, G. Raffelt, and M. Rampp, Astrophys. J. **587**, 320 (2003).
[25] A. Burrows and R. F. Sawyer, Phys. Rev. C **58**, 554 (1998); **59**, 510 (1999).
[26] C. J. Horowitz, Phys. Rev. D **65**, 043001 (2002).
[27] G.W. Carter and M. Prakash, Phys. Lett. B **525**, 249 (2002).
[28] J. M. Lattimer and F. D. Swesty, Nucl. Phys. **A535**, 331 (1991); J. M. Lattimer, C. J. Pethick, D. G. Ravenhall, and D. Q. Lamb, Nucl. Phys. **A432**, 646 (1985).
[29] S. E. Woosley, A. Heger, and T. A. Weaver, Rev. Mod. Phys. **74**, 1015 (2002).
[30] D. Lai and P. Goldreich, Astrophys. J. **535**, 402 (2000).
[31] A. Heger *et al.* (to be published).
[32] W. Keil, H.-T. Janka, and E. Müller, Astrophys. J. Lett. **473**, L111 (1996).
[33] K. Langanke *et al.*, astro-ph/0302459.
[34] S. Akiyama, J. C. Wheeler, D. L. Meier, and I. Lichtenstadt, Astrophys. J. **584**, 954 (2003).